

In vivo electron donation from plastocyanin and cytochrome c 6 to PSI in Synechocystis sp. PCC6803

Stefania Viola, Julien Sellés, Benjamin Bailleul, Pierre Joliot, Francis-André Wollman

▶ **To cite this version:**

Stefania Viola, Julien Sellés, Benjamin Bailleul, Pierre Joliot, Francis-André Wollman. In vivo electron donation from plastocyanin and cytochrome c 6 to PSI in Synechocystis sp. PCC6803. Biochimica biophysica acta (BBA) - Bioenergetics, 2021, 1862 (9), pp.148449. 10.1016/j.bbabio.2021.148449 . hal-03280323

HAL Id: hal-03280323
https://hal.sorbonne-universite.fr/hal-03280323

Submitted on 7 Jul 2021

HAL is a multi-disciplinary open access archive for the deposit and dissemination of scientific research documents, whether they are published or not. The documents may come from teaching and research institutions in France or abroad, or from public or private research centers.

L'archive ouverte pluridisciplinaire **HAL**, est destinée au dépôt et à la diffusion de documents scientifiques de niveau recherche, publiés ou non, émanant des établissements d'enseignement et de recherche français ou étrangers, des laboratoires publics ou privés.

In vivo electron donation from plastocyanin and cytochrome c_6 to PSI in *Synechocystis* sp. PCC6803

Stefania Viola[a,b], Julien Sellés[a], Benjamin Bailleul[a], Pierre Joliot[a], Francis-André Wollman,[1,a]

[a]Chloroplast Biology and Light-sensing in Microalgae-UMR7141, IBPC, CNRS-Sorbonne Université, Paris, France.
[b]Department of Life Sciences, Imperial College – South Kensington Campus, London, UK.

[1]Corresponding author: Francis-André Wollman
Address: UMR7141 - IBPC, 13 rue Pierre et Marie Curie, 75005 Paris, France
Tel: +33 (0)1 58 41 50 12
Email: wollman@ibpc.fr

Author contributions: S.V., B.B., J.S., P.J. and F.A.W. designed the experiments; S.V., B.B., J.S. and P.J. performed the experiments; S.V., B.B., J.S., and P.J. analysed the data; S.V. wrote the manuscript, and B.B., J.S., P.J. and F.A.W. reviewed it.

The authors declare no conflict of interest.

Highlights

- Both plastocyanin and cytochrome c_6 form a pre-complex with photosystem I in *Synechocystis*
- Fast electron donation to PSI occurs from both plastocyanin and cytochrome c_6
- The extent of formation of the pre-complex in the dark is not affected by respiration
- Electron partitioning between respiration and photosynthesis is regulated in a similar way in presence of either of the two electron donors

Abstract

Many cyanobacteria species can use both plastocyanin and cytochrome c_6 as lumenal electron carriers to shuttle electrons from the cytochrome b_6f to either photosystem I or the respiratory cytochrome *c* oxidase. In *Synechocystis* sp. PCC6803 placed in darkness, about 60% of the active PSI centres are bound to a reduced electron donor which is responsible for the fast re-reduction of P_{700} *in vivo* after a single charge separation. Here, we show that both cytochrome c_6 and plastocyanin can bind to PSI in the dark and participate to the fast phase of P_{700} reduction, but the fraction of pre-bound PSI is smaller in the case of cytochrome c_6 than with plastocyanin. Because of the inter-connection of respiration and photosynthesis in cyanobacteria, the inhibition of the cytochrome *c* oxidase results in the over-reduction of the photosynthetic electron transfer chain in the dark that translates into a lag in the kinetics of P_{700} oxidation at the onset of light. We show that this is true both with plastocyanin and cytochrome c_6, indicating that the partitioning of electron transport between respiration and photosynthesis is regulated in the same way independently of which of the two lumenal electron carriers is present, although the mechanisms of such regulation are yet to be understood.

Keywords: Cyanobacteria, Photosystem I, Plastocyanin, Cytochrome c_6, Respiration

1- Introduction

In oxygenic photosynthesis, electrons extracted from water are transported from the photosystem II (PSII) donor side (thylakoid lumen) to the photosystem I (PSI) acceptor side (stroma / cytoplasm) via a third transmembrane complex, the cytochrome b_6f (cyt b_6f). Cyt b_6f takes electrons from the membrane-soluble plastoquinone pool and passes them to an electron acceptor soluble in the lumenal space, which in turn reduces P_{700}, the PSI chlorophyll that gets stably oxidised after charge separation. In higher plants this soluble electron carrier is, in most cases, a copper-containing protein named plastocyanin, whereas a c-type cytochrome named cytochrome c_6 (cyt c_6) can replace plastocyanin as a lumenal electron donor to PSI in many algae and cyanobacteria (1). It should be noted that cytochrome c_6 is present also in plants, but its functional equivalence to plastocyanin has not yet been demonstrated (2, 3). Both plastocyanin and cyt c_6 are small (ca. 10 kDa) monomeric proteins with a redox potential of about +350 mV at pH 7. This redox potential is close to the one of cytochrome *f* (4), the cyt b_6f subunit from which they accept electrons, but it is lower than the one of P_{700}, that ranges between +400 and +470 mV depending on the organism (5, 6). If plastocyanin from plants and algae are acidic proteins, plastocyanin and cytochrome c_6 can have widely different isoelectric point values in cyanobacteria (1).

The electron transfer kinetics between plastocyanin / cyt c_6 and PSI have been investigated extensively in eukaryotes. *In vitro* studies have shown the existence, after a saturating light flash, of a fast ($t_{½}$ of few µs) electron transfer phase responsible for the reduction of P_{700} in ~30-40% of isolated PSI particles from both plants (7) and green algae (8). Such a fast phase also has been measured in intact plant chloroplasts and green algae cells (7, 9, 10). Thus, P_{700} re-reduction kinetics are bi-phasic, with the fast phase pointing to the fraction of PSI centres to which is bound, in the dark prior to the light flash, a reduced electron donor. The slower phase corresponds to the diffusion time of plastocyanin / cyt c_6 in the lumenal space to PSI centres that do not have any pre-associated electron donor. In the case of the eukaryotic PSI, the PsaF subunit has been shown to carry the binding site for the transient electron carrier-PSI complex (8, 11), with a crucial role played by its lumenal N-terminal extension, rich in Lysine residues. These positive residues would electrostatically interact with the acidic surface of the electron donor, thus providing a high affinity binding site. In a *Chlamydomonas reinhardtii* mutant carrying a deletion of this N-terminal extension, the P_{700} reduction kinetics proved to be slower than in the wild type (12). In contrast to the chloroplast-located PsaF, the PsaF subunit of cyanobacterial PSI lacks the Lysin-rich lumenal extension. Together with the observation that some species have basic plastocyanin or cyt c_6 isoforms, this sequence change in the cyanobacterial version of PsaF suggests that electrostatic interactions might not be the main factor determining their interaction with PSI in cyanobacteria. Rather, the presence of conserved Tryptophan residues on the lumenal side of the PsaA and PsaB PSI core subunits in both cyanobacteria (13) and algae (14, 15) suggests an hydrophobic interaction mechanism, since these residues were shown to be pivotal for the binding of plastocyanin and cyt c_6,.

The existence of a fast phase of electron transfer to PSI in cyanobacteria has been a matter of debate. *In vitro* studies using *Synechocystis* sp. PCC6803, showed that electron donation from either plastocyanin or cyt c_6 to the endogenous PSI displays monophasic kinetics, with a half-time intermediate between those from the two phases described in chloroplasts (16). Consistent with these data, plastocyanin and cyt c_6 from *Anabaena* sp. PCC7119, as well as plastocyanin isolated from *Synechocystis* sp. PCC6803, cannot quickly donate electrons to spinach PSI.

However the reduction of P_{700} in PSI particles from *Anabaena* displays a fast phase with cyt c_6, but not with plastocyanin, from the same organism (17). P_{700} reduction kinetics comprising a fast phase also have been observed *in vivo* in conditions where only cyt c_6 is used as PSI electron donor: this is the case in the cyanobacteria *Plectonema boryanum* (18), in a thermophilic *Synechococcus* sp. (19, 20) and in *Synechococcus* sp. PCC 7002 (21). Recently we have shown the existence *in vivo* of such a fast phase in *Synechococcus elongatus* sp. PCC7942 and *Synechocystis* sp. PCC6803 (22), grown in BG11 medium containing 0,5 µM Cu, in conditions which favour expression of plastocyanin (23, 24). In these cyanobacteria, which harbour both the genes coding for plastocyanin and cyt c_6, the expression of the two electron donors is indeed regulated according to the availability of the metals used as cofactors, iron and copper. Using *Synechocystis* sp. PCC6803 wild type grown in presence of different metal concentrations and in mutant strains for either plastocyanin or cyt c_6, the two proteins have been shown to be functional electron carriers in both the photosynthetic and the respiratory chains (23, 25, 26), which are located and interconnected in the same cyanobacterial thylakoids (reviewed in 24, 25). In these organisms, once reduced by the cyt b_6f, plastocyanin and cyt c_6 can donate electrons to both PSI and Cytochrome *c* Oxidase (COX) (29, 30). Cyanobacteria possess an *aa3*-type COX enzyme, using two haems and three copper atoms as cofactors (31). The most oxidising cofactors of COX (CuB, +412 mV at pH 6.5 in *Paracoccus denitrificans* (32)) and of PSI (P_{700}, between +400 and +470 mV) have similar redox potentials, providing similar driving forces for electron donation from plastocyanin and cyt c_6. However, the determinants of the *in vivo* kinetic competition between the two pathways are still unknown, limiting our understanding of the competition between the respiratory and photosynthetic flows. Here, we present a detailed *in vivo* analysis of the electron donation kinetics from either plastocyanin or cyt c_6 to PSI, in the wild type strain *Synechocystis* sp. PCC6803 (hereafter referred to as *Synechocystis*) and in a mutant devoid of plastocyanin and expressing cyt c_6 instead. We also address the possible influence of the respiratory activity on such kinetics.

2- Materials and Methods

2.1- Cyanobacteria Cultures

Synechocystis sp. PCC6803 cells were grown under white light (30-35 µmol photons/m^2/s) at 25°C in BG11 medium (containing 0.5 µM Cu and 20 µM Fe, pH 8.0) with constant shaking. For the generation of the *Synechocystis* ΔPC mutant, all DNA techniques such as plasmid isolation, restriction and ligation were performed according to standard protocols (33). All the enzymes used here were purchased from New England Biolabs. A 1405 bp long region encompassing the *petE* gene (SYNPCCP_2261) was amplified from *Synechocystis* sp. PCC6803 genomic DNA using the primers SacI-petE FW (5'-aatataGAGCTCAACCACCGTTATCAGCAGAAC, SacI restriction site underlined, non-genomic sequence in small letters) and EcoRI-petE RV (5'-aatataGAATTCCTACTCTATTTAACCATCTGTATATCGAGG, EcoRI restriction site underlined, non-genomic sequence in small letters). The fragment was gel-purified and digested with the restriction enzymes SacI and EcoRI and subsequently ligated into the plasmid pSBA2 (34) previously digested with the same enzymes. The plasmid was then linearized with the enzymes SmaI and HpaI and ligated with a blunt-ended kanamycin resistance cassette (Kan^R). The resulting plasmid in which part of the *petE* gene was replaced by the resistance cassette was sequenced and introduced into the wild-type *Synechocystis* strain, and transformants were selected on increasing concentrations of kanamycin. Completely segregated ΔPC mutant clones were obtained and verified by PCR using the primer pairs SacI-petE FW + petE del RV (5'- TTTAGACATACTTCTTGGCGATTG, specific for the wild-type allele) and SacI-petE FW + KanR RV (5'- ATGTAAGCCCACTGCAAGCTAC, specific for the Kan^R-containing allele).

The ΔPC mutant was maintained in presence of 100 µg/ml kanamycin. When used for measurements, cells were grown in absence of kanamycin, harvested by centrifugation in the mid exponential phase of growth, resuspended in their own supernatant to the appropriate concentration and incubated in the same conditions as for growth for at least one hour before starting the experiments.

2.2- Inhibitors and redox mediators

3-(3,4-dichlorophenyl)-1,1-dimethylurea (DCMU) was dissolved in ethanol; hydroxylamine (HA), 5-Methylphenazinium methyl sulphate (PMS), potassium cyanide (KCN) and methyl viologen (MV) were dissolved in water; rotenone (Rot) was dissolved in DMSO. PSII inhibition was achieved using 20 µM DCMU and 500 µM HA. PMS was used at a final concentration of 15 µM, KCN at 50 µM, MV at 300 µM and Rot at 50 µM.

2.3- Whole-cell absorption spectra

These were determined with a Cary 300 UV-VIS spectrophotometer (Varian). Spectra were recorded from 400 to 750 nm and normalized to the absorption at 630 nm.

2.4- Protein analyses

All steps of protein extraction were performed at 4° C. Cells in exponential growth phase were harvested by centrifugation, washed once in ice-cold PBS buffer, re-suspended in 1/400

volumes of ice-cold PBS containing protease inhibitors (cOmplete EDTA-free, Roche) and mixed with 2/3 volumes of glass beads (425-600 µm, acid-washed, Sigma). Cells were broken by subsequent cycles of freezing/thawing and vortexing. Glass beads were sedimented by a brief slow-speed centrifugation and the total cell extract (T) recovered in the supernatant. Half volume of the total cell extract was centrifuged at 16000 rcf for 30 minutes and the supernatant was recovered as the soluble fraction (S), whereas the pellet, corresponding to the membrane fraction (M) was washed once in PBS and finally resuspended in the same PBS volume as the soluble fraction. The chlorophyll concentration of the whole cell extract and membrane fraction was calculated according to (35). Whole cell extracts and membrane protein samples were adjusted to the same chlorophyll concentration, whereas soluble protein samples were adjusted on a volume basis (same as the corresponding membrane sample). Proteins were denatured by boiling in presence of 3% SDS, 100 mM DTT and 100 mM Na_2CO_3 and then loaded (3 µg Chl *a* per lane) on a 4-20% SDS-PAGE gel (TGX Mini gel, BioRad). After electrophoresis, proteins were transferred by semi-dry blotting on a nitrocellulose membrane (Amersham Protran 0.1 µm NC, GE Helthcare). For c-type haem detection, the membrane was rinsed in PBS and immediately incubated with ECL (Clarity Western ECL Blotting Substrate, BioRad). For immunodetection, the membrane was saturated with 5% milk proteins in PBS-T and immuno-decorated with primary antibodies, diluted 10 000-fold (PsbA and plastocyanin, Agrisera), then revealed by horseradish peroxidase–conjugated antibodies against rabbit IgG (Promega). Signals were detected by ECL using the ChemiDoc Imager (BioRad).

2.5- Spectroscopy measurements

For all spectroscopic measurements, several experimental traces recorded on the same biological material were averaged until a satisfying signal-to-noise ratio was achieved. All the data shown in this work are therefore averages of several experimental traces, the number depending on the signal quality of each individual trace (typically around 10).

A home-made Optical Parametric Oscillator (OPO)-based spectrophotometer (36) with a time resolution of 10 ns and a spectral resolution of 2 nm was used for the pump-probe and pump-pump-probe measurements of section 3.2. Cells were injected in two closed horizontal cuvettes, one used as a reference (without actinic light) and the other used for measurement with actinic light. In this setup, detecting flashes are split between the two cuvettes and monitored carefully in order to avoid actinic effects, whereas the actinic light illuminates only one of the two. The cells were incubated in the cuvettes in presence of specified inhibitors in the dark for at least 30 minutes before the experiments, in anaerobic conditions. The actinic flashes were provided by one or two Nd:YAG lasers at 532 nm which pumped an OPO producing monochromatic saturating flashes at 690 nm. The absorption changes induced by these actinic flashes were sampled at discrete times by short detecting flashes generated by another OPO. The time delay between the laser delivering the actinic flashes and the laser delivering the detecting flashes was controlled by a digital delay/pulse generator (DG645, Stanford Research). The light-detecting photodiodes were protected from transmitted and scattered actinic light and fluorescence of the samples by BG39 Schott (Mainz, Germany) filters. The pump-pump-probe measurements of PSI re-reduction kinetics were performed as described in (22). In this setup,

the maximal P_{700}^{+} levels were measured as the *ΔI/I* 435 nm at 200 ns after a single-turnover flash in presence of the PSII inhibitors DCMU and HA.

A LED-based spectrophotometer (JTS10, Biologic, France) was used for measurements of absorbance change kinetics in the >100 µs time range. Cells were injected in a closed horizontal cuvette in presence of the specified inhibitors and measurements were performed in presence and absence of actinic illumination on each biological sample. The absorption changes induced by the measuring light alone (actinic effects or changes in the LED output intensity due to heating) were then subtracted from those recorded in presence of actinic illumination. In this setup the cells were kept in aerobic conditions by manual re-oxygenation every few minutes. Actinic flashes were provided by a dye laser at 690 nm, whereas multi-turnover light pulses were provided by a red LED array. For measurements in the 540 – 573 nm region, measuring pulses were provided by a converted green LED (Unicolor Converted Green OSTAR Projection Cube, OSRAM Opto Semiconductor) using appropriate interference filters (10 nm full width at half-maximum, Edmund Optics). P_{700} redox changes were measured through the difference of the absorbance changes at 705 and 730 nm using measuring pulses provided by a combination of red LEDs and appropriate interference filters. The light-detecting diodes were protected from scattered actinic light by a BG39 filter (Schott) for measurements in the 540 – 573 nm region and by a RG695 (Schott) filter for P_{700} measurements. In this setup, the maximal P_{700}^{+} levels were measured as the maximal *ΔI/I* 705 – 730 nm obtained during a multi-turnover saturating pulse in presence of the PSII inhibitor DCMU and of methyl viologen.

3- Results

3.1- Generation and characterization of the Synechocystis ΔPC mutant

We generated the *Synechocystis* plastocyanin deficient strain by partially replacing the endogenous *petE* gene (from position -158 to position +180 with respect to the start of the coding sequence) with a kanamycin resistance cassette, as shown in Fig. 1A (see section 2.1 for details). The complete segregation of the ΔPC mutant clones was verified by PCR (Fig. 1B). Clone number 3 (from now on indicated as ΔPC) was used for further analyses. The whole cell absorption spectra (Fig. 1C) revealed only minor differences between the wild type and the ΔPC mutant, with a slightly lower Chl *a* (peaks at 440 and 682 nm) to phycocyanin (peak at 630 nm) ratio in the latter, as previously reported (37). Both the wild-type and ΔPC strains were grown photoautotrophically in unmodified BG11 medium, containing 0,5 µM Cu: at this Cu concentration *Synechocystis* wild-type cells express mostly the copper-based plastocyanin with only low levels of the alternative electron transporter cyt c_6 (23). Indeed, when performing protein analyses (Fig. 1D) the wild type displayed a large amount of plastocyanin but little cyt c_6 (compare its haem signal to that of cyt *f* in the total cell extract). It must be noted that we cannot exclude that the faint signal present in the wild type that we attribute to cyt c_6 could rather correspond to another c-type cytochrome of comparable size, as for example the cytochrome c_M. This cytochrome has been detected in *Synechocystis* cells grown at 30°C (38) and its expression has been shown to increase when cells are grown at room temperature (39), as in the present work.

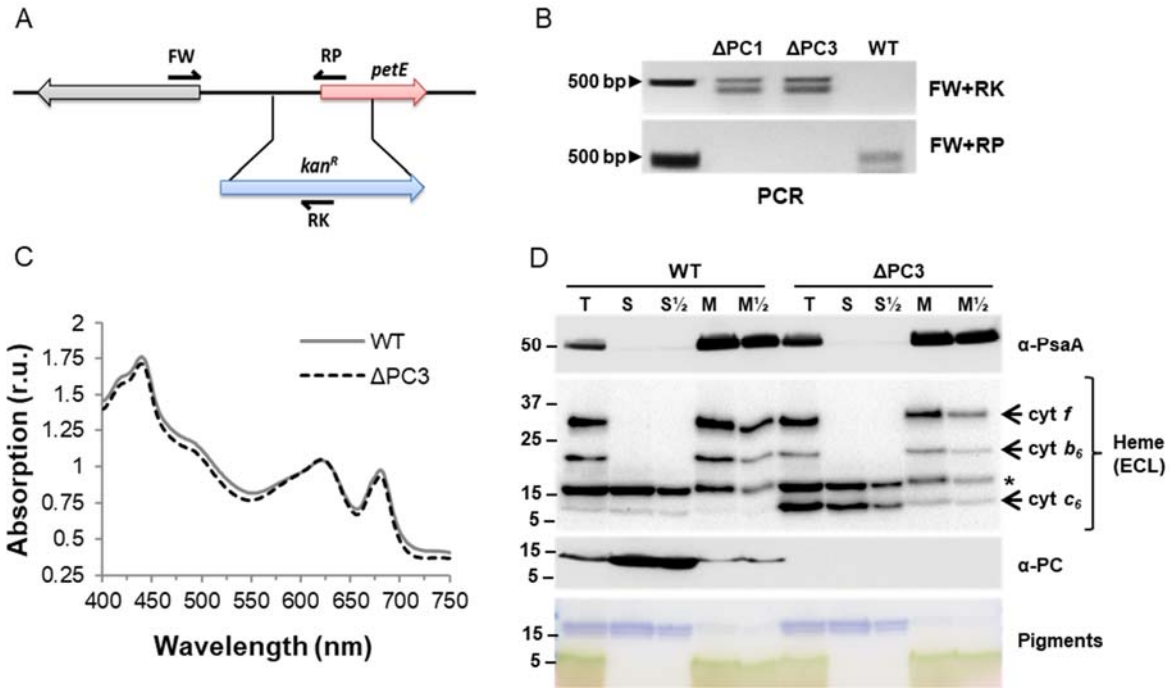


Fig. 1. Generation and characterization of the *Synechocystis* ΔPC mutant. (A) Schematic representation of the partial replacement of the *petE* gene with the kanamycin resistance cassette (kan^R) in the ΔPC mutant strain. FW (SacI-petE FW), RP (petE del RV) and RK (KanR RV) are the primers used for genotyping. (B) PCR-based genotyping, using the primers depicted in (A), of two independent ΔPC

clones, including the WT as control. (C) Absorption spectra of WT and ΔPC (clone 3) cells, normalized on the absorption at 630 nm. (D) Analysis of protein accumulation in total cell extracts (T), soluble fractions (S) and membrane fractions (M) of WT and ΔPC (clone 3) cells. Proteins were separated on 4-18 % SDS-PAGE gels and then transferred to nitrocellulose membranes. Proteins were either detected by immuno-decoration (antibodies against the PsaA subunit of PSI and against plastocyanin, PC) or by the reaction of ECL with c-type haems. The asterisk indicates a non-assigned protein band present in both WT and mutant. The pigments running at the front of the gel (phycobilisome pigments and Chl *a*) were used as markers of the cell fractions.

Since the identity of this cytochrome is not particularly relevant for our study, in the following we will refer to it as cyt c_6 for economy. In contrast, the ΔPC strain expressed no plastocyanin but much higher amounts of cyt c_6 than the wild type. Both proteins were mostly found in soluble fractions and their low amounts in the membrane fractions can be attributed to a minor contamination from soluble proteins, evident also in the distribution of the phycobiliproteins. Although the relative changes in the amounts of each of the two transporters are clear when comparing the two strains, we could not quantify their absolute amounts per cell, owing to the lack of protein standards. The plastocyanin deficient mutant did not display any significant differences in the accumulation of either PSI or cyt b_6f with respect to the wild type, as also confirmed by Clear Native-PAGE analysis of the membrane fractions (Fig. S1C).

In order to get a semi-quantitative estimation of the levels of cyt c_6 expressed in the ΔPC mutant, we spectroscopically determined the ratio between the c-type cytochromes and P_{700}. To ensure a full oxidation of all c-type cytochromes and P_{700}, we used a saturating light pulse (high oxidation rate) in presence of the PSII inhibitors 3-(3,4-dichlorophenyl)-1,1-dimethylurea (DCMU) and hydroxylamine (HA) to prevent their reduction by electrons extracted from PSII. The time-resolved absorption changes were recorded between 545 and 573 nm (Fig. 2), where stand the α bands of all cytochromes (21). These absorption changes were measured during a 1.5 s illumination with a strong (1000 µmol photons/m^2/s) red light and they were normalized to the maximal P_{700}^+ signal ($\Delta I/I$ 705-730 nm) measured in the same conditions. A linear regression between the $\Delta I/I$ at 545 and at 573 nm was set as baseline. It must be noted that in these measurements, performed using the JTS10 spectrophotometer, the wavelengths of the measuring pulses are selected using interference filters (10 nm full width at half-maximum), so the spectral resolution is lower than the one obtained when using the OPO-based spectrophotometer, as in section 3.2. As shown in Fig. 2, the amplitude of the bleaching corresponding to the oxidation of cytochromes was about three times larger in the ΔPC mutant than in the wild type after 1.5 s illumination. In the latter, the signal corresponded predominantly to the oxidation of cytochrome *f* from the cyt b_6f complex, whereas the bleaching corresponded to the oxidation of both cyt *f* and cyt c_6 in the ΔPC mutant. Indeed, the peak in the absorption changes in the latter was blue shifted by two nm – 554 nm versus 556 nm- in agreement with the spectral differences previously reported for the two cytochromes (21). By measuring in different cultures the maximal bleach corresponding to c-type cytochrome oxidation with respect to the maximal bleach at 700 nm due to P_{700} oxidation, we determined that the ΔPC mutant accumulates 3.2±0.3 (3 replicates) times more c-type cytochromes per PSI than the wild type. Since we observed no significant differences in the

cyt *f*/PSI ratio at the protein level between the two strains (Fig 1), the additional bleaching measured in the mutant must be ascribed to the accumulation of oxidized cyt c_6. Taken together, these observations point to the presence of about two cyt c_6 molecules per cyt b_6f monomer in the ΔPC mutant. The spectroscopic detection of cyt c_6 accumulation levels were similar in the ΔPC clones 1 and 3, as shown in Fig. S1. It must be noted that the spectra recorded in the wild type also presented an unusual broadening towards the shortest wavelengths with respect to a pure cytochrome *f* spectrum. This is in line with the biochemical observation that small amounts of cyt c_6 are present in addition to plastocyanin and thus contribute to the overall bleach.

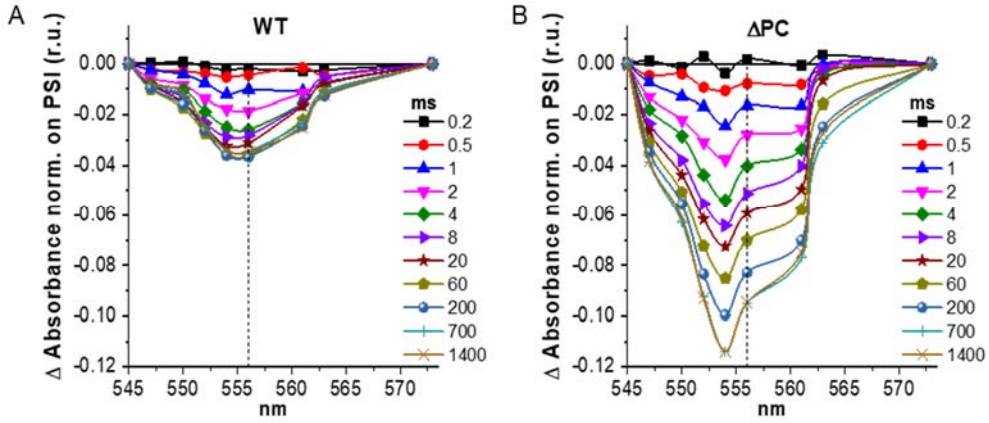


Fig. 2. Time-resolved accumulation of oxidized c-type cytochromes in *Synechocystis* WT (A) and ΔPC (B) cells. Absorption changes were measured in presence of DCMU and HA at the indicated times (in ms) after the onset of a 1.5 s illumination with a strong red actinic light and normalized on total P_{700}^+ (maximal *ΔI/I* 705-730 nm measured at the end of the light pulse). The linear regression between *ΔI/I* 545 and *ΔI/I* 573 nm was set as baseline for each recording time. The dotted vertical lines mark the 556 nm wavelength.

3.2- Flash-induced in vivo kinetics of plastocyanin/cyt c_6-dependent electron donation to PSI

We then investigated kinetics of the redox changes on these c-type cytochromes after a single turnover saturating flash. These were measured in presence of DCMU and HA in the α-band region of c-type cytochromes (Fig. 3A and B, traces recorded in biological replicates are shown in Fig. S2A and B). These measurements were performed using the OPO-based spectrophotometer, having a spectral resolution of 2 nm. The spectra were normalized on the total P_{700}^+ signals, and the baseline calculation was done as described above for Fig. 2. In the wild type, the bleaching appearing with a peak at 556 nm corresponds for the major part to the oxidation of cyt *f*. Again, a small shoulder around 550-552 nm could be observed, corresponding to the small amounts of cyt c_6 present in this strain. The relative amplitude of this shoulder is lower in the spectra in Fig. S2A with respect to those in Fig. 3A, suggesting variable cyt c_6 amounts in the different cultures. In the ΔPC mutant the bleaching peaking at 553 nm has a maximal amplitude twice as large as in the wild type. This is because the charge is shared by cyt c_6 and cyt *f* in the mutant, whereas in the wild type it is shared between cyt *f* and plastocyanin that does not contribute to the absorption changes in this region. The kinetics of the absorption changes in the 550-558 nm region are shown in Fig. 3C and D (and Fig. S2C

and D): in the wild type the kinetics were very similar at all wavelengths, as they are dominated by the absorption changes due to cytochrome *f*, which gets oxidised with a t½ of ~200 µs. A minor faster bleach is visible in the 100 µs time range at 550-552 nm: this likely corresponds to the fast oxidation of the small amounts of cyt c_6 present. In the ΔPC mutant the kinetics were more complex, clearly showing a faster bleaching at 550-554 nm and a slower one at 556-558 nm. Therefore, the oxidation of cyt c_6, mostly responsible for the *ΔI/I* 550-554 nm, preceded the one of cyt *f*, that has a major contribution in the *ΔI/I* 556-558 nm. From the above kinetics we estimate that cyt c_6 oxidation occurs with a t½ of ~20 µs, indicative of a fast electron donation to PSI.

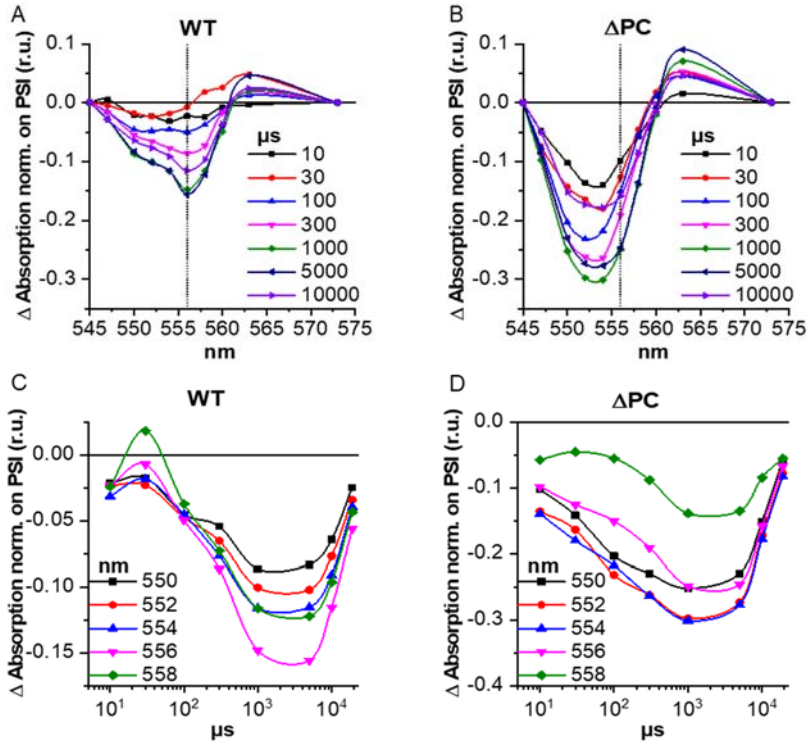


Fig. 3. Flash-induced oxidation and reduction kinetics of c-type cytochromes in *Synechocystis* WT (A and C) and ΔPC (B and D) cells. (A) and (B) Absorption changes were measured in presence of DCMU and HA at the indicated times (in µs) after a single-turnover saturating flash and normalized on total PSI (*ΔI/I* 435 nm measured at 200 ns after the flash), and the linear regression between *ΔI/I* 545 and *ΔI/I* 573 nm was set as baseline for each recording time. (C) and (D) Kinetics of the absorption changes between 550 and 580 nm from panels A and B.

In a previous study (22) we have shown that the re-reduction of oxidized P_{700} after a single-turnover saturating flash is bi-phasic *in vivo* in the wild type strain of *Synechocystis*: it displays a fast phase that corresponds to electron donation by a pre-fixed plastocyanin (or possibly cyt c_6, in a small fraction of PSI centres) and a slow phase which accounts for the diffusion time of additional electron donors in the thylakoid lumen. We thus investigated the kinetics of electron donation from cyt c_6 to PSI in the ΔPC mutant, following the same approach as in (22) which is based on ElectroChromic Shift (ECS) measurements. The light-induced ECS signal that can be measured as *ΔI/I* (500-485nm) in *Synechocystis*, is proportional to the electric field generated by charge separations within each photosystem. The amplitude of the ECS signal

measured within 1 ms after a single-turnover saturating flash given in presence of PSII inhibitors (DCMU and HA) corresponds to one charge separation per active PSI. During a few milliseconds after the flash, the positive charge originally present on P_{700}^+ is stabilized on secondary electron donors on the lumenal side of PSI, thus maintaining the trans-membrane electric field but allowing another charge separation within the PSI reaction centres in which P_{700} has been re-reduced. It follows that the fraction of PSI centres whose P_{700} has been reduced by a soluble donor at a given time after the first flash can be measured through the increase in ECS generated by a second flash. In our experimental conditions, where the cells were incubated in anaerobiosis and darkness for at least one hour before starting the measurements, the transmembrane electric field generated by the single flash remained quite stable in the 5 ms time range and any decay was taken into account (see Fig. S3 for further explanations). The advantage of using ECS instead of P_{700}^+ absorption spectroscopy is that the evolution between the two flashes allows us to discriminate between charge recombination and electron transfer from plastocyanin / cyt *c*$_6$. Both charge recombination and electron transfer from secondary donors will translate into a reduction of P_{700}. The ECS discriminates the two processes: charge recombination will suppress the electric field generated by the first flash whereas electron transfer from plastocyanin / cyt *c*$_6$ to P_{700} will keep the electric field constant. Therefore, we measured the *in vivo* kinetics of P_{700} reduction by secondary donors in the wild type and in the ΔPC strains as described above (Fig.4 A, B and C). The fitted experimental traces are shown individually in Fig. S4. As expected, the kinetics in the wild type were bi-phasic, with about 60% of P_{700} being re-reduced in less than 100 μs ($t_{½}$ ~10 μs). A fast phase with similar kinetics ($t_{½}$ ~15 μs) was observed also in the case of the ΔPC mutant, although the fraction of P_{700} reduced in less than 100 μs was only about 30% of the total. The fast re-reduction kinetics of P_{700} in the ΔPC strains correspond very well to the cyt *c*$_6$ oxidation kinetics measured in the same conditions (Fig. 3D). In both strains the fast P_{700} reduction phase was followed by a considerably slower phase, with about 20 and 40 % of the total P_{700} still remaining oxidized 5 ms after the first flash in the wild type and the mutant, respectively.

In order to promote the full re-reduction of P_{700} in the time during which the electric field generated by the first charge separation is preserved (few ms), we used the redox mediator PMS. PMS accepts electrons from PSI on the stromal/cytoplasmic side and when it gets doubly-reduced and protonated it partitions inside the lumen and donates electrons to P_{700}, likely via plastocyanin or cyt *c*$_6$ (40), while releasing protons. In our previous work (22) we demonstrated that the presence of PMS did not affect the fraction of PSI centres in which P_{700} was reduced during the fast (100 μs) phase but it shortened the slow phase of reduction. This suggests that PMS should not donate electrons directly to PSI fast enough to outcompete electron donation from the pre-fixed plastocyanin or cytochrome *c*$_6$. Indeed, the addition of PMS did not significantly change the kinetics of the fast phase in either of the two strains (Table S1), while it considerably accelerated the slow reduction phase, leading to the full re-reduction of P_{700} within 5 ms. These conditions allowed us to confirm that the ECS signal in the ΔPC mutant is linearly proportional to the electric field, as previously demonstrate for the wild type (22). These results indicate that a secondary donor is pre-bound in the dark to a fraction of PSI in both the wild-type and the mutant strain. This fast-donating electron carrier is either plastocyanin (plus traces of cyt *c*$_6$) in the wild type or cytochrome *c*$_6$ in the ΔPC mutant, the latter case involving a much smaller fraction of the PSI centres.

In order to further confirm that the fast P_{700} reduction phase corresponds to the electron donation from a lumenal donor to PSI and is not due to a direct donation from PMS, we measured in the same conditions as above the kinetics of the absorption changes at 416 nm. At this wavelength, light-induced absorption changes measured in presence of PSII inhibitors contain a P_{700}^+ contribution mixed with an ECS contribution and with the absorption peaks of oxidized cytochromes in the Soret region (21). We have previously shown (22) that PMS strongly suppresses the oxidation of cytochrome *f* induced by a single-turnover flash, thus eliminating its contribution from the flash-induced absorption changes at 416 nm. Consequently, the wild type incubated with PMS should display only a minor contribution from cyt c_6 oxidation on top of P_{700} redox changes and ECS, whereas in the case of the ΔPC mutant, one would expect an additional contribution coming from cyt c_6 oxidation, unless PMS by-passes it and re-reduces P_{700} directly. As shown in Fig. 4D, the absorption kinetics at 416 nm in the ΔPC mutant indeed were very different from those in the wild type: in the latter the bleaching was maximal at 200 ns after the flash (corresponding to the maximal P_{700} oxidation and to the rapid rise phase of ECS) and it relaxed steadily (see inset Fig. 4D), whereas in the mutant, owing to cyt c_6 oxidation, the bleaching further increased during the first 100 µs, before relaxing. This confirms that PMS does not by-pass cyt c_6 during the fast phase, which thus gets oxidized by PSI before getting re-reduced. Although we do not have experimental data showing the oxidation of plastocyanin in the wild type under the same circumstances, we assume that it occurs in the same way, given the very similar redox potentials of the two lumenal electron carriers.

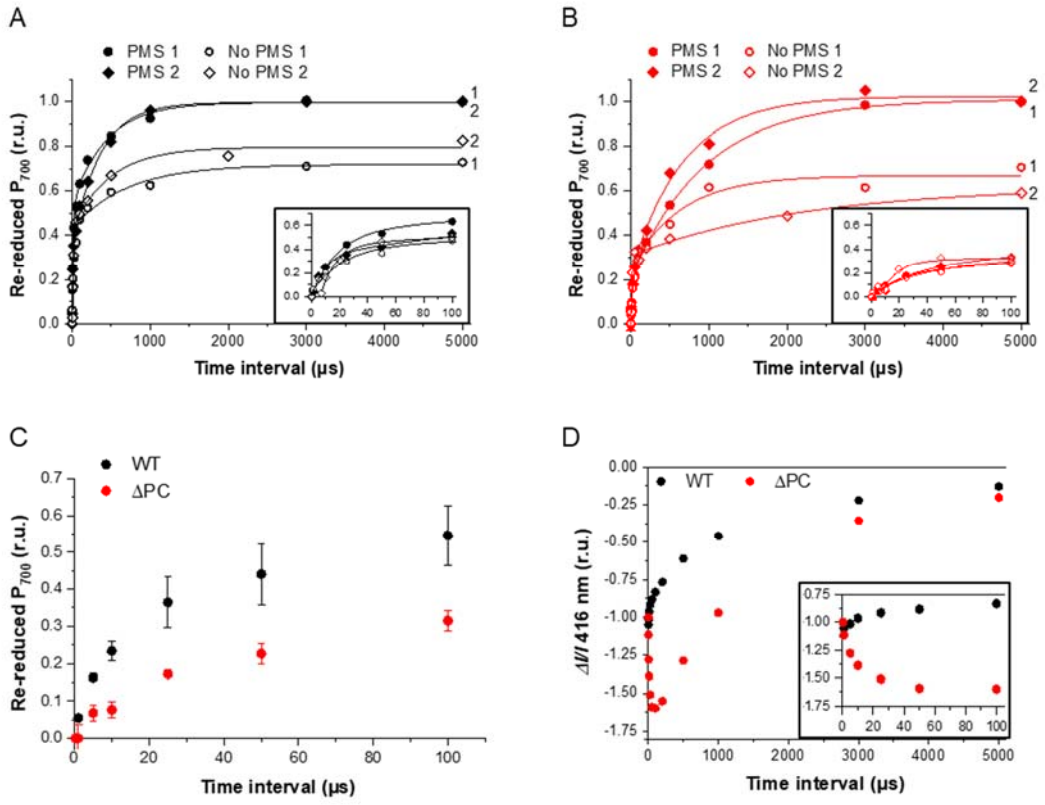


Fig. 4. Electron transfer kinetics between secondary electron donors and PSI in *Synechocystis*. (A) and (B) P_{700}^+ re-reduction kinetics measured in WT and ΔPC cells, respectively, in presence of DCMU and

HA with (closed symbols, two biological replicates) and without (open symbols, two biological replicates) PMS, using the double-flash ECS method (ECS measured as *ΔI/I* 500 - 485 nm, time interval between two saturating flashes expressed in µs). The inserts represent the first 100 µs with an expanded scale. The two exponential fits of the experimental data are represented by the continuous lines. (C) Averaged (±s.d.) kinetics of the WT and ΔPC P_{700} re-reduction fast phase in panels A and B. (D) Flash-induced absorption changes measured at 416 nm in presence of DCMU, HA and PMS. Absorption changes were sampled at the indicated time intervals after the flash (in µs) and normalized on the absorption change measured at 200 ns after the flash. The insert represents the first 100 µs with an expanded scale.

3.3- Partitioning of the intersystem electron fluxes in presence of plastocyanin or cyt c_6

In cyanobacteria, as already mentioned in the introduction, plastocyanin and cyt c_6 can donate electrons to both PSI and the respiratory cytochrome oxidase complex, COX. The partitioning between the photosynthetic and respiratory flows at this intersection should depend on the affinity of the plastocyanin or cytochrome c_6 for PSI or COX but the modalities of this partitioning are still unresolved in cyanobacteria. This aspect was irrelevant to the previous experiments since the kinetics of electron donation from plastocyanin/cyt c_6 to PSI after a single-turnover flash reported above were measured in anaerobic conditions. In absence of oxygen, COX is not functional and therefore cannot compete for electrons with PSI. In the following, we maintained the cells in aerobic conditions by frequent mixing and reinjection in the sample cuvette to investigate whether the *in vivo* partitioning of electrons between PSI and COX depends on the molecular nature of the electron donor in *Synechocystis*. To this aim, we measured the P_{700} oxidation-reduction kinetics upon single or multiple turnover illumination in the presence of DCMU - to prevent re-reduction of P_{700} by PSII - and of various combinations of: i) potassium cyanide (KCN), an inhibitor of COX (29); ii) methyl viologen, serving as artificial PSI acceptor (41); and iii) rotenone (Rot), that inhibits the activity of the NADPH dehydrogenase complex (NDH), thus also blocking one of the pathways of electron injection in the intersystem electron carriers (42). All P_{700} traces were normalized to the total PSI amounts present in each sample, measured as the maximal *ΔI/I* (705 – 730) nm obtained at the end of a multi-turnover light pulse in presence of DCMU and methyl viologen (MV).

First, we investigated if the fraction of pre-bound PSI secondary donors is affected by COX activity, using single turnover flashes (Fig. 5). In the kinetics of P_{700} reduction, the first point was recorded 100 µs after the flash: at this time, about 60% of P_{700} in the wild type and 20% in the ΔPC mutant were already re-reduced, no matter which inhibitors or mediators were present.

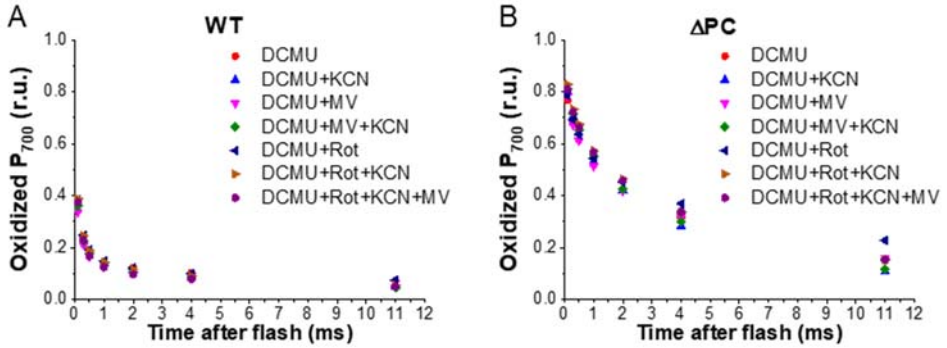


Fig. 5. P_{700}^+ kinetics (*ΔI/I* 705-730 nm) measured in *Synechocystis* WT (A) and ΔPC (B) cells measured after a single-turnover saturating flash (first measuring time 100 µs after the flash) in presence of DCMU and various combinations of: methyl viologen (MV), Rotenone (Rot) and potassium cyanide (KCN). All traces are normalized to the total PSI present in each sample (maximal *ΔI/I* 705-730 nm measured during a 75 ms light pulse in presence of DCMU and MV). The flash was applied at time-point 0.

This is consistent with the ECS-based kinetics of P_{700} reduction reported above in anaerobic conditions, which suggests that the fraction of pre-bound electron donor in the dark depends neither on the redox state of the intersystem electron carriers nor on the activity of the COX. The inhibition of COX by KCN did not modify the fraction of rapidly reduced P_{700}, further confirming that the pre-bound fraction does not depend on a competition between the affinity of plastocyanin / cyt *c6* for PSI and for COX, in the dark. This also demonstrates that in our experimental conditions KCN did not lead to Cu removal from plastocyanin, as had been previously reported in broken chloroplasts, at a much higher KCN concentrations than the 50 µM used here (43).

To investigate the electron partitioning between PSI and COX in the light, we used instead multi turnover pulses, again in presence of DCMU and aerobic conditions. The addition of the COX inhibitor KCN strongly prevented the full oxidation of P_{700} during a short (75 ms) saturating pulse, in a similar way in both strains (Fig. 6A and C). When applying longer pulses of lower intensity light (Fig. 6B and D showing traces recorded in independent cultures with respect to those used for panels A and C), an almost complete oxidation of P_{700} could be reached even in presence of KCN, although the oxidation kinetics remained much slower than in its absence. In addition, the P_{700} reduction kinetics at the light offset (time-point 0) were faster in presence of KCN+DCMU than with DCMU alone with both short and long pulses. Since in presence of DCMU no electrons coming from PSII are injected in the intersystem electron transport chain, the lag in P_{700} oxidation during illumination and the faster reduction at the light offset induced by KCN suggest that the inhibition of the COX results in: i) a transitory higher rate of cyclic electron flow (CEF), ii) a transient acceptor side limitation of PSI resulting in charge recombination, or iii) a combination of both (44). Independently of the process behind the lag in P_{700} oxidation in presence of KCN, the inhibition of COX led to an accumulation of reduced PSI electron donors and/or acceptors prior to and during illumination.

In dark-adapted *Arabidopsis* leaves the P_{700}^+ decay at the offset of a saturating light pulse comprises a fast phase which is completed in 1 ms and is attributed to $P_{700}^+A_1^-$ charge recombination within PSI (48). Since the P_{700} reduction kinetics that we measured in *Synechocystis* did not show a faster reduction phase completed in 1 ms (Fig. 6), it is tempting to suggest that the KCN-induced faster reduction of P_{700} is due to a faster cyclic electron flow around PSI. However, we cannot fully exclude a role of charge recombination involving the reduced terminal PSI iron-sulphur clusters F_A and F_B: as reviewed in (49), charge recombination between P_{700}^+ and $(F_A/F_B)^-$ has been shown to occur over tens of milliseconds in isolated plant PSI particles. Such recombination may occur *in vivo* in absence of available ferredoxin, were it detached from PSI centres or over-reduced upon inhibition of the respiratory chain in presence of KCN. Charge recombination could especially contribute to the strong lag in P_{700} oxidation that we observed during the first tens of ms of the multiple turnover pulses (Fig. 6A, B, C and D) in presence of KCN. The fact that P_{700}^+ absorption spectroscopy cannot

easily distinguish between cyclic electron flow and charge recombination has been recently discussed in experiments with *C. reinhardtii*, where up to half of the PSI charge separations measured with this method during the first hundreds of milliseconds of illumination in dark-adapted cells were attributed to charge recombination rather than to an actual electron flow (44). However, there is one situation where the contribution of charge recombination can be neglected compared to CEF. This is at the end of the long pulse (Fig. 6 B and D), when P_{700} is almost fully oxidized: the acceptor side limitation is absent in these conditions. The re-reduction rates of P_{700} are still faster in the presence of KCN than in its absence which indicates that CEF is promoted by the inhibition of the COX.

KCN could lead to PSI over-reduction not only via the inhibition of COX but also by inhibiting the Calvin-Benson cycle, as shown for example in (45). Such an inhibition could result in both PSI acceptor side limitation and an increase in CEF. However, a COX-specific effect of KCN was revealed by the effect of an addition of 300 µM methyl viologen. This addition counteracted the KCN-induced acceleration of the P_{700} reduction kinetics at the end of the long pulse (Fig. 6 B and D), which is easily interpreted by the competition of MV for the electrons used in the CEF promoted by the presence of KCN. Besides competing for electrons with CEF, MV has also been shown to efficiently prevent charge recombination in PSI (41). Despite these two effects, its addition did not fully prevent the lag in P_{700} oxidation induced by KCN during a short pulse and during the initial phase of illumination when applying a longer pulse (see Fig. S5 for details). This can be explained by the accumulation of electrons on the donor side of PSI prior to illumination because of the inhibition of COX.

It must be noted that KCN also inhibits the cyanobacterial plastoquinone terminal oxidase Cyd. However at a 50 µM concentration, as used here, COX is fully inhibited whereas part of Cyd remains active (46). Nonetheless, a partial inhibition of Cyd could contribute to the accumulation of reduced PSI donors/acceptors that we observe in presence of KCN. In accordance with this, a retardation in P_{700} oxidation upon illumination and its faster re-reduction at the light offset have been previously reported in a *Synechocystis* mutant devoid of COX and even more markedly in a mutant devoid of both COX and Cyd (47).

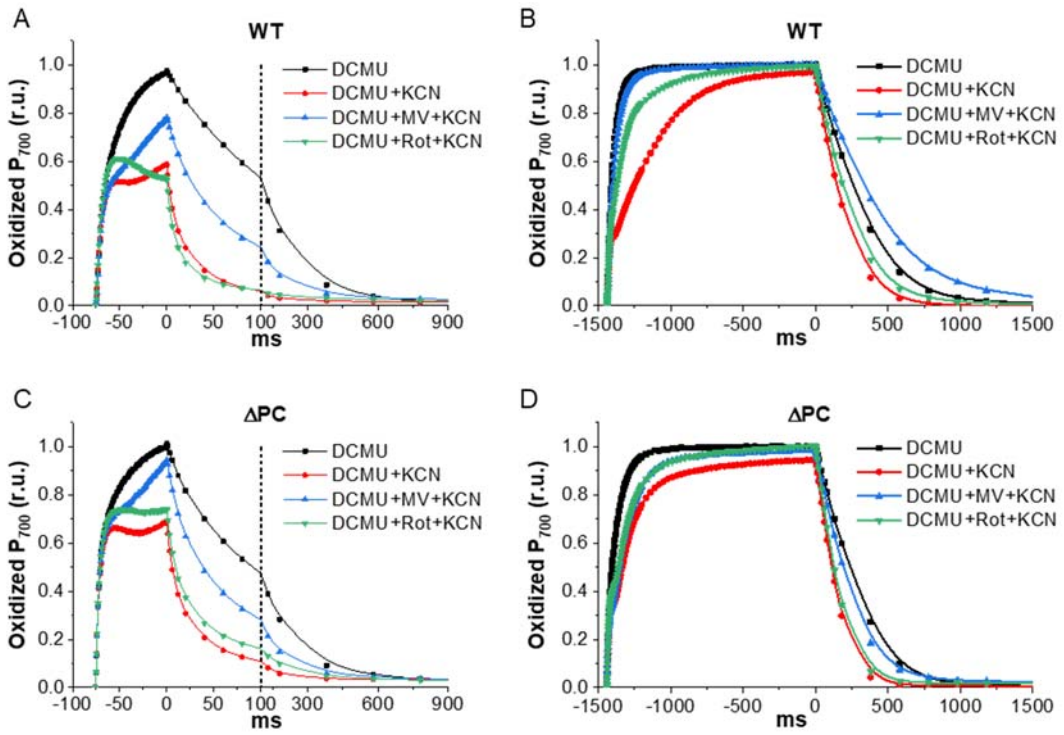


Fig. 6. P_{700}^{+} kinetics (*ΔI/I* 705-730 nm) measured in *Synechocystis* WT (A and B) and ΔPC (C and D) cells in presence of DCMU and various combinations of: methyl viologen (MV), Rotenone (Rot) and potassium cyanide (KCN). All traces are normalized to the total PSI present in each sample (maximal *ΔI/I* 705-730 nm measured at the end of a light pulse in presence of DCMU and MV). (A) and (C) P_{700}^{+} kinetics measured during short (75 ms) pulses of saturating light (2500 µmol photons/m^2/s). The dashed lines indicate a change of scale in the time (ms) axis. (B) and (D) P_{700}^{+} kinetics measured during long (1.5 s) pulses of strong light (1200 µmol photons/m^2/s). In all panels, the time-point 0 is at the pulse offset. Cells used in panels (A) and (C) were the same as those used in Fig. 5, while cells used in panels (B) and (D) are from independent cultures.

In cyanobacteria, one of the entry points of electrons in the intersystem chain is represented by the NDH complex, which accepts electrons from stromal reductants and re-injects them upstream of PSI at the level of the plastoquinone pool. This pathway can be inhibited by rotenone (42). Addition of this inhibitor partially relieved the P_{700} over-reduction induced by KCN during illumination and it did not significantly slow down the fast PSI re-reduction at the offset of the light pulse (Figure 6). The effect of rotenone, although limited, points to the availability, in presence of KCN, of a higher pool of electron donors to PSI in part maintained by the activity of the NDH. The fact that rotenone counteracted only partly the effect of KCN on the redox changes of P_{700} during the pulses can be explained by the fact that it does not prevent charge recombination and by the presence of a NDH-independent cyclic pathway in cyanobacteria (50).

In conclusion, the response of the oxidation and reduction kinetics of P_{700} to the inhibitors and mediator used here were similar in the wild type and ΔPC strains.

4- Discussion

We have shown that in *Synechocystis* wild type grown in normal BG11 the electron carrier plastocyanin is expressed preferentially, although some cytochrome c_6 is also present, in line with previous literature (see section 3.1). Upon deletion of the gene encoding plastocyanin the cells accumulate cytochrome c_6 instead.

The *in vivo* reduction kinetics of P_{700} after a single-turnover flash is bi-phasic with either plastocyanin or cytochrome c_6 as electron donor (Fig. 4). Both these donors can thus pre-bind in the dark to PSI and can reduce the P_{700}^+ formed upon illumination with comparable kinetics (t½ ~10-15 µs). Very convincingly, the kinetics of cyt c_6 oxidation after a flash (t½ slightly higher than 10 µs, see Fig 3B) is similar to the fast phase of the kinetics of P_{700} reduction in the ΔPC mutant. We showed that even in presence of PMS the fast P_{700} reduction phase after a flash represents an electron transfer from a pre-bound plastocyanin / cyt c_6 to PSI. In our results, though, the slower phase of P_{700} reduction was PMS-sensitive and we cannot exclude that PMS could compete with lumenal electron donors for a direct P_{700} reduction in the hundreds of µs to ms time scale. In presence of PMS we could indeed observe a fast flash-induced oxidation of cyt c_6 in the ΔPC mutant, completed in 100 µs, corresponding to the fast electron donation to PSI centres forming a pre-complex, followed by a re-reduction having t½ ~1.5 ms (Fig 4D). Such re-reduction kinetics are well suited to account for the slow P_{700}^+ reduction phase observed in the same conditions (Fig. 4B), which could suggest that cyt c_6 does mediate electron donation from PMS to PSI. Nonetheless, PMS could at the same time donate electrons directly to PSI, as it is known to do *in vitro* when no other soluble electron carrier is present (see for example (51)). This could especially be true if the diffusible lumenal electron carriers were present in sub-stoichiometric amounts compared to PSI, as discussed below.

The fraction of PSI centres having a pre-bound electron donor is lower in the ΔPC mutant than in the wild type (~30% and ~60% of the total, respectively). Using spectroscopy, we estimated the presence of about two cytochrome c_6 molecules per cytochrome b_6f complex in the mutant (Fig. 2) but we know neither the concentration of cyt c_6, nor that of plastocyanin in the wild type, relatively to PSI. The difference in the fraction of PSI centres having a pre-bound electron donor observed in the two strains could reflect a difference in the total amount of lumenal donors, with the cyt c_6/PSI ratio being lower in the ΔPC mutant than the plastocyanin/PSI ratio in the wild type. However, it is of note that the correlation between the amount of the sole plastocyanin relative to PSI and the amplitude of the fast P_{700} reduction phase varies in plant chloroplasts. Indeed, in spinach chloroplast a plastocyanin/PSI ratio of ~3 resulted in the reduction of almost all P_{700}^+ in tens of µs (52), whereas in *Arabidopsis* leaves the amount of P_{700} reduced in 100 µs was reported to be ~60% even in overexpressor lines accumulating a large excess of plastocyanin (53). Another comparative *in vitro* study performed with isolated particles from plants, green algae and cyanobacteria (17) described a fast P_{700} reduction phase, the amplitude of which depended on species and on the molecular nature of the electron donor (plastocyanin or cyt c_6). Therefore, the differences in the fraction of P_{700} reduced in 100 µs in the wild type and ΔPC mutant could also be in part due to changes in the affinity of the electron donor to the PSI binding site.

In isolated PSI particles from *Chlamydomonas* the amplitude, but not the kinetics, of the fast P_{700} reduction phase has been shown to be dependent on the concentration of the soluble electron donor, were it plastocyanin or cytochrome c_6 (8). Our results could therefore be accounted for if cytochrome c_6 has the same properties of electron donation to PSI as plastocyanin, but that it remains sub-stoichiometric with respect to PSI in the ΔPC strain.

Indeed, in the flash-induced kinetics of cytochrome oxidation in absence of PMS, we observed that the oxidation of cytochrome c_6 is mostly completed in 100 µs, when only 30% of P_{700} is reduced (Fig. 3 and Fig. S2). This suggests that most of the available cyt c_6 is oxidised during this phase. Therefore, we suggest that the stoichiometry of lumenal donor per PSI would be of ~0.6 for plastocyanin versus ~0.3 for cytochrome c_6. This is consistent with the higher proportion of P_{700} remaining oxidised in the ΔPC mutant, 5 ms after a single-turnover flash, when no PMS is present (Fig. 4B). A plastocyanin/PSI ratio of ~1.3 has been recently measured in *Synechocystis* cells by near-infrared spectroscopy (54). In our study the cells are grown at lower temperature and lower light intensity than in (54), which could explain the discrepancy in the estimated ratios since the expression of the *petE* gene has been shown to be affected by both factors (39). Sub-stoichiometric amounts of soluble cytochromes relative to PSI have been previously reported in a thermophilic *Synechococcus sp.* in which plastocyanin was absent (55). Based on spectroscopy results (Fig. 2) we estimated that in the ΔPC mutant the cyt b_6f amounts are about half of the cyt c_6 ones, which would result in a cyt b_6f per PSI stoichiometry of ~0.15. These quantitative estimates, that are not meant to be precise, are not in disagreement with the literature, where cyt b_6f to PSI ratios as low as 0.2 have been reported, varying in function of the cyanobacterial species analysed and the growth conditions (56–58).

In both the wild type and the ΔPC mutant the percentage of PSI centres having in the dark a pre-bound electron donor was comparable whether the cytochrome *c* oxidase is active or inhibited by KCN in aerobic conditions and it did not change either when switching to anaerobic conditions (compare Fig. 4A and B and Fig. 5). Therefore, despite the fact that COX, as PSI, relies on plastocyanin and cytochrome c_6 as electron donors, their oxidation in the dark via respiration does not affect the fraction that is pre-bound to the lumenal side of PSI, as if the two donor systems were not in competition.

Either of the three following hypothesis could account for these observations : i) the concentration ratio of COX to PSI in *Synechocystis* thylakoids is so low that the activity of COX as a negligible effect on the amount of electron donors available for PSI; ii) PSI and COX are connected to two physically separated pools of cytochrome b_6f and lumenal donors; or iii) PSI and COX are connected to the same pool of electron donors, but in the dark the affinity of reduced plastocyanin or cyt c_6 for PSI is so high that none of the pre-bound electron donors are available as COX substrates. Although there are no reports of an actual quantification of the COX/PSI ratio in the literature, the localization of COX in the thylakoids membranes of cyanobacteria is well documented (31, 59, 60), as are the effects of its inhibition (61) or absence (30, 46) on the photosynthetic electron transport. In our experiments, the inhibition of COX with KCN resulted in a marked lag in P_{700} oxidation during short saturating light pulses and at the onset of longer pulses (Fig. 6). These results rule out hypothesis i), as they imply that in our experimental samples COX was present in sufficient amounts to maintain, in absence of KCN, the electron transport chain upstream of PSI in a more oxidised state than in presence of the inhibitor.

The inhibition of COX thus results in a larger pool of PSI electron donors available prior to illumination, but it does not increase the proportion of PSI centres that have a pre-bound donor. This observation can be equally well accounted for by hypotheses ii) or iii). If there were distinct PSI and COX domains, still there would be diffusion-limited electron transfer from cyt b_6f complexes closely associated to either PSI or COX. The inhibition of COX would strongly affect the P_{700} oxidation kinetics upon illumination, because the two electron transfer chains

would still be connected through the plastoquinone pool, that would get over-reduced in presence of KCN. A spatial segregation of COX in cyanobacteria thylakoids has not been experimentally demonstrated, but such a segregation was reported for the respiratory complexes NDH and succinate dehydrogenase (62). Alternatively, if PSI and COX rely on a shared pool of electron donors but with a much higher affinity of PSI for the electron donors in darkness, these would partition differently in the dark and under illumination: in the dark the partitioning of donors between PSI and COX mainly depends on their relative affinity, whereas upon illumination the availability of luminal donors becomes diffusion-limited. It also has been suggested that the light-induced changes in the ionic strength of the lumen could favour association of plastocyanin or cyt c_6 with COX, while their association with PSI would be favoured in the dark (63). However, such a switch mechanism has not yet been demonstrated *in vivo*.

Independently of the underlying model, though, we have shown that the *in vivo* partitioning of electrons between PSI and COX upon multi-turnover illumination is rather insensitive to whether the lumenal electron carrier is plastocyanin or cyt c_6. Indeed, in both cases the inhibition of COX activity results in the accumulation of electrons in the photosynthetic chain, resulting in a lag in the oxidation of P_{700} at the dark-to-light transition. Our results could not discriminate between the role of cyclic electron flow and of charge recombination in inducing the lag, although it is very likely that both processes were involved. Indeed, the transient over-reduction of the intersystem chain induced by the inhibition of COX activity would also result in the over-reduction of the cytoplasmic pool of PSI acceptors (ferredoxin, FNR and $NADP^+$). Reduced ferredoxin is the electron donor of the NDH complex (64), which in turn injects electrons in the plastoquinone pool (42, 65). In both our strains the inhibition of NDH with rotenone partially relieved the P_{700} over-reduction induced by KCN during light pulses (Fig. 6), thus confirming that the NDH activity was in part responsible for the dark reduction of the photosynthetic chain. This indicates that the lag in P_{700} oxidation induced by the inhibition of COX was not solely due to charge recombination. The NDH has been shown to play a role, together with the flavodiiron (Flv) proteins, in regulating the redox homeostasis of the photosynthetic chain (66). Nonetheless, we show here that when the electron flux towards oxygen mediated by COX is inhibited, the NDH and Flv activities are not sufficient to prevent a transient over-reduction of P_{700} during the first tens of milliseconds of the dark to high light transition. This observation confirms the role of respiratory oxidases to prevent photodamage, as it has been previously shown in *Synechocystis* cultures subjected to a growth regime characterized by rapid dark-to-high light transitions (30).

The present study provides further experimental evidence that plastocyanin and cyt c_6 are functionally equivalent in *Synechocystis in vivo*, with respect the photosynthetic and respiratory chains. The functional interaction between these two metabolic chains is far from being understood, but further time-resolved analysis of the partitioning of electron transport between respiration and photosynthesis in light-dark cycles should provide key information in that respect.

Acknowledgments
This work was supported by UMR7141, CNRS/ Sorbonne Université, by the Agence Nationale

de la Recherche (ReCyFuel: ANR-16-CE05-0026-01) and by the LabEx DYNAMO (ANR-11-LABX-0011-01). We thank Bill Rutherford for useful discussions.

Bibliography

1. Díaz-Quintana A, et al. (2003) A comparative structural and functional analysis of cyanobacterial plastocyanin and cytochrome c_6 as alternative electron donors to Photosystem I: Photosystem I reduction in cyanobacteria. Photosynth Res 75(2):97–110.
2. Wastl J, Bendall DS, Howe CJ (2002) Higher plants contain a modified cytochrome c_6. Trends Plant Sci 7(6):244–245.
3. Gupta R, He Z, Luan S (2002) Functional relationship of cytochrome c_6 and plastocyanin in Arabidopsis. Nature 417(6888):567–571.
4. Alric J, Pierre Y, Picot D, Lavergne J, Rappaport F (2005) Spectral and redox characterization of the heme ci of the cytochrome b_6f complex. Proc Natl Acad Sci 102(44):15860–15865.
5. Sétif P, Leibl W (2007) Chapter 14. Functional pattern of Photosystem I in oxygen evolving organisms, pp 147–191.
6. Nakamura A, Suzawa T, Kato Y, Watanabe T (2011) Species dependence of the redox potential of the primary electron donor P_{700} in photosystem I of oxygenic photosynthetic organisms revealed by spectroelectrochemistry. Plant Cell Physiol 52(5):815–823.
7. Bottin H, Mathis P (1985) Interaction of plastocyanin with the photosystem I reaction center: a kinetic study by flash absorption spectroscopy. Biochemistry 24(23):6453–6460.
8. Hippler M, Drepper F, Farah J, Rochaix JD (1997) Fast electron transfer from cytochrome c_6 and plastocyanin to photosystem I of *Chlamydomonas reinhardtii* requires PsaF. Biochemistry 36(21):6343–6349.
9. Haehnel W, Hesse V, Pröpper A (1980) Electron transfer from plastocyanin to P_{700}. Function of a subunit of photosystem I reaction center. FEBS Lett 111(1):79–82.
10. Delosme R (1991) Electron transfer from cytochrome *f* to photosystem I in green algae. Photosynth Res 29(1):45–54.
11. Farah J, Rappaport F, Choquet Y, Joliot P, Rochaix JD (1995) Isolation of a psaF-deficient mutant of *Chlamydomonas reinhardtii*: efficient interaction of plastocyanin with the photosystem I reaction center is mediated by the PsaF subunit. EMBO J 14(20):4976–4984.
12. Hippler M, Drepper F, Haehnel W, Rochaix JD (1998) The N-terminal domain of PsaF: Precise recognition site for binding and fast electron transfer from cytochrome c_6 and plastocyanin to photosystem I of *Chlamydomonas reinhardtii*. Proc Natl Acad Sci U S A 95(13):7339–7344.
13. Sun J, et al. (1999) Oxidizing side of the cyanobacterial photosystem I. Evidence for interaction between the electron donor proteins and a luminal surface helix of the PsaB subunit. J Biol Chem 274(27):19048–19054.

14. Sommer F, Drepper F, Hippler M (2002) The luminal helix l of PsaB is essential for recognition of plastocyanin or cytochrome c_6 and fast electron transfer to photosystem I in *Chlamydomonas reinhardtii*. J Biol Chem 277(8):6573–6581.
15. Sommer F, Drepper F, Haehnell W, Hippler M (2004) The hydrophobic recognition site formed by residues PsaA-Trp651 and PsaB-Trp627 of Photosystem I in *Chlamydomonas reinhardtii* confers distinct selectivity for binding of plastocyanin and cytochrome c_6. J Biol Chem 279(19):20009–20017.
16. Hervás M, Ortega JM, Navarro JA, De la Rosa MA, Bottin H (1994) Laser flash kinetic analysis of *Synechocystis* PCC 6803 cytochrome c_6 and plastocyanin oxidation by Photosystem I. BBA - Bioenerg 1184(2–3):235–241.
17. Hervás M, Navarro JA, Díaz A, Bottin H, De la Rosa MA (1995) Laser-flash kinetic analysis of the fast electron transfer from plastocyanin and cytochrome c_6 to photosystem I. Experimental evidence on the evolution of the reaction mechanism. Biochemistry 34(36):11321–11326.
18. Hiyama T, Ke B (1971) Laser-induced reactions of P_{700} and cytochrome *f* in a blue-green alga, *Plectonema boryanum*. BBA - Bioenerg 226(2):320–327.
19. Nanba M, Katoh S (1983) Reaction kinetics of P-700, cytochrome c-553 and cytochrome *f* in the cyanobacterium, *Synechococcus* sp. BBA - Bioenerg 725(2):272–279.
20. Nanba M, Katoh S (1985) Electron transport from cytochrome b_6f complexes to Photosystem I reaction center complexes in *Synechococcus* sp. Is cytochrome c-553 a mobile electron carrier? BBA - Bioenerg 808(1):39–45.
21. Baymann F, Rappaport F, Joliot P, Kallas T (2001) Rapid electron transfer to photosystem I and unusual spectral features of cytochrome c_6 in *Synechococcus* sp. PCC 7002 *in vivo*. Biochemistry 40(35):10570–10577.
22. Viola S, et al. (2019) Probing the electric field across thylakoid membranes in cyanobacteria. Proc Natl Acad Sci U S A 116(43):21900–21906.
23. Zhang L, Mcspadden B, Pakrasi HB, Whitmarsh J (1992) Copper-mediated regulation of cytochrome c553 and plastocyanin in the cyanobacterium *Synechocystis* 6803. J Biol Chem 267(27):19054–19059.
24. Clarke AK, Campbell D (1996) Inactivation of the *petE* gene for plastocyanin lowers photosynthetic capacity and exacerbates chilling-induced photoinhibition in the cyanobacterium *Synechococcus*. Plant Physiol 112(4):1551–1561.
25. Durán R V., Hervás M, De La Rosa MA, Navarro JA (2004) The efficient functioning of photosynthesis and respiration in *Synechocystis* sp. PCC 6803 strictly requires the presence of either cytochrome c_6 or plastocyanin. J Biol Chem 279(8):7229–7233.
26. Ardelean I, Matthijs HCP, Havaux M, Joset F, Jeanjean R (2002) Unexpected changes in photosystem I function in a cytochrome c_6-deficient mutant of the cyanobacterium *Synechocystis* PCC 6803. FEMS Microbiol Lett 213(1):113–119.
27. Mullineaux CW (2014) Co-existence of photosynthetic and respiratory activities in cyanobacterial thylakoid membranes. Biochim Biophys Acta - Bioenerg 1837(4):503–511.

28. Lea-Smith DJ, Bombelli P, Vasudevan R, Howe CJ (2016) Photosynthetic, respiratory and extracellular electron transport pathways in cyanobacteria. Biochim Biophys Acta - Bioenerg 1857(3):247–255.
29. Howitt CA, Vermaas WFJ (1998) Quinol and cytochrome oxidases in the cyanobacterium *Synechocystis* sp. PCC 6803. Biochemistry 37(51):17944–17951.
30. Lea-Smith DJ, et al. (2013) Thylakoid terminal oxidases are essential for the cyanobacterium *Synechocystis* sp. PCC 6803 to survive rapidly changing light intensities. Plant Physiol 162(1):484–495.
31. Peschek BGA, Molitor VIR, Trnka M (1988) Characterization of cytochrome-c oxidase in isolated and purified plasma and thylakoid membranes from cyanobacteria. Methods Enzymol 167:437–449.
32. Gorbikova EA, Vuorilehto K, Wikström M, Verkhovsky MI (2006) Redox titration of all electron carriers of cytochrome c oxidase by Fourier transform infrared spectroscopy. Biochemistry 45(17):5641–5649.
33. Sambrook, J., Fritsch, E.F. and Maniatis, T. (1989) Molecular Cloning. New York, NY: Cold Spring Harbor Laboratory Press.
34. Lagarde D, Beuf L, Vermaas W (2000) Increased production of zeaxanthin and other pigments by application of genetic engineering techniques to *Synechocystis* sp. strain PCC 6803. Appl Environ Microbiol 66(1):64–72.
35. Porra RJ, Thompson WA, Kriedemann PE (1989) Determination of accurate extinction coefficients and simultaneous equations for assaying chlorophylls a and b extracted with four different solvents: verification of the concentration of chlorophyll standards by atomic absorption spectroscopy. Biochim Biophys Acta 975:384–394.
36. Joliot P, Béal D, Rappaport F (1998) A new high-sensitivity 10-ns time-resolution spectrophotometric technique adapted to in vivo analysis of the photosynthetic apparatus. Review of Scientific Instruments 70(202):4247–4252.
37. Wang XQ, Jiang HB, Zhang R, Qiu BS (2013) Inactivation of the *petE* gene encoding plastocyanin causes different photosynthetic responses in cyanobacterium *Synechocystis* PCC 6803 under light-dark photoperiod and continuous light conditions. FEMS Microbiol Lett 341(2):106–114.
38. Cho YS, Pakrasi HB, Whitmarsh J (2000) Cytochrome cM from *Synechocystis* 6803. detection in cells, expression in *Escherichia Coli*, purification and physical characterization. Eur J Biochem 267(4):1068–1074.
39. Malakhov MP, Malakhova OA, Murata N (1999) Balanced regulation of expression of the gene for cytochrome c(M) and that of genes for plastocyanin and cytochrome c_6 in *Synechocystis*. FEBS Lett 444(2–3):281–284.
40. Forti G, Rosa L (1971) On the pathway of electron transport in cyclic photophosphorylation. FEBS Lett 18(1):55–58.
41. Sétif P (2015) Electron-transfer kinetics in cyanobacterial cells: Methyl viologen is a poor inhibitor of linear electron flow. Biochim Biophys Acta - Bioenerg 1847(2):212–222.
42. Mi H, Endo T, Schreiber U, Ogawa T, Asada K (1994) NAD(P)H dehydrogenase-dependent cyclic electron flow around photosystem-I in the cyanobacterium

Synechocystis PCC-6803 - A Study of dark-starved cells and spheroplasts. Plant Cell Physiol 35(2):163–173.
43. Berg SP, Krogmann DW (1975) Mechanism of KCN inhibition of photosystem I. J Biol Chem 250(23):8957–8962.
44. Nawrocki WJ, et al. (2019) Maximal cyclic electron flow rate is independent of PGRL1 in *Chlamydomonas*. Biochim Biophys Acta - Bioenerg 1860(5):425–432.
45. Kobayashi Y, Heber U (1994) Rates of vectorial proton transport supported by cyclic electron flow during oxygen reduction by illuminated intact chloroplasts. Photosynth Res 41(3):419–428.
46. Pils D, Schmetterer G (2001) Characterization of three bioenergetically active respiratory terminal oxidases in the cyanobacterium *Synechocystis* sp. strain PCC 6803. FEMS Microbiol Lett 203(2):217–222.
47. Ermakova M, et al. (2016) Distinguishing the roles of thylakoid respiratory terminal oxidases in the cyanobacterium *Synechocystis* sp. PCC 6803. Plant Physiol 171(2):1307–1319.
48. Joliot P, Béal D, Joliot A (2004) Cyclic electron flow under saturating excitation of dark-adapted Arabidopsis leaves. Biochim Biophys Acta - Bioenerg 1656(2–3):166–176.
49. Brettel K (1997) Electron transfer and arrangement of the redox cofactors in photosystem I. Biochim Biophys Acta - Bioenerg 1318(3):322–373.
50. Yeremenko N, et al. (2005) Open reading frame *ssr2016* is required for antimycin A-sensitive photosystem I-driven cyclic electron flow in the cyanobacterium *Synechocystis* sp. PCC 6803. Plant Cell Physiol 46(8):1433–1436.
51. Schlodder E, Çetin M, Byrdin M, Terekhova I V., Karapetyan N V. (2005) P_{700}^{+}- and $^{3}P_{700}$-induced quenching of the fluorescence at 760 nm in trimeric Photosystem I complexes from the cyanobacterium *Arthrospira platensis*. Biochim Biophys Acta - Bioenerg 1706(1–2):53–67.
52. Haehnel W, Ratajczak R, Robenek H (1989) Lateral distribution and diffusion of plastocyanin in chloroplast thylakoids. J Cell Biol 108(4):1397–1405.
53. Pesaresi P, et al. (2009) Mutants, overexpressors, and interactors of Arabidopsis plastocyanin isoforms: Revised roles of plastocyanin in photosynthetic electron flow and thylakoid redox state. Mol Plant 2(2):236–248.
54. Theune ML, et al. (2021) In-vivo quantification of electron flow through photosystem I – Cyclic electron transport makes up about 35% in a cyanobacterium. Biochim Biophys Acta - Bioenerg 1862(3):148353.
55. Aoki M, Hirano M, Takahashi Y, Katoh S (1983) Contents of cytochromes, quinones and reaction centers of photosystems I and II in a cyanobacterium *Synechococcus* sp. Plant Cell Physiol 24(3):517–525.
56. Murakami A, Kim SJ, Fujita Y (1997) Changes in photosystem stoichiometry in response to environmental conditions for cell growth observed with the cyanophyte *Synechocystis* PCC 6714. Plant Cell Physiol 38(4):392–397.
57. Zorz JK, et al. (2015) The RUBISCO to photosystem II ratio limits the maximum photosynthetic rate in picocyanobacteria. Life 5(1):403–417.

58. Casella S, et al. (2017) Dissecting the native architecture and dynamics of cyanobacterial photosynthetic machinery. Mol Plant 10(11):1434–1448.
59. Peschek GA, et al. (1989) Characterization of the cytochrome c oxidase in isolated and purified plasma membranes from the cyanobacterium *Anacystis nidulans*. Biochemistry 28(7):3057–3063.
60. Peschek GA, Obinger C, Fromwald S, Bergman B (1994) Correlation between immuno-gold labels and activities of the cytochrome-c oxidase (aa3-type) in membranes of salt stressed cyanobactria. FEMS Microbiol Lett 124(3):431–437.
61. Cooley JW, Vermaas WFJ (2001) Succinate dehydrogenase and other respiratory pathways in thylakoid membranes of *Synechocystis* sp. strain PCC 6803: Capacity comparisons and physiological function. J Bacteriol 183(14):4251–4258.
62. Liu LN, et al. (2012) Control of electron transport routes through redox-regulated redistribution of respiratory complexes. Proc Natl Acad Sci U S A 109(28):11431–11436.
63. Nicholls P, Obinger C, Niederhauser H, Peschek GA (1991) Cytochrome c and c-554 oxidation by membranous *Anacystis nidulans* cytochrome oxidase. Biochem Soc Trans 19(3):991.
64. Schuller JM, et al. (2019) Structural adaptations of photosynthetic complex I enable ferredoxin-dependent electron transfer. Science (80-) 363(6424):257–260.
65. Mi H, Endo T, Schreiber U, Ogawa T, Asada K (1992) Electron donation from cyclic and respiratory flows to the photosynthetic intersystem chain is mediated by pyridine nucleotide dehydrogenase in the cyanobacterium *Synechocystis* PCC 6803. Plant Cell Physiol 33(8):1233–1237.
66. Nikkanen L, et al. (2020) Functional redundancy between flavodiiron proteins and NDH-1 in *Synechocystis* sp. PCC 6803. Plant J 103:1460–1476.